A combined Analytical Experimental and Numerical Investigation of Turbulent Air Flow Behaviour in a Rotor-Stator cavity

Fadi Abdel Nour, Sébastien Poncet, Roger Debuchy, Gérard Bois

A Combined Analytical, Experimental and Numerical Investigation of Turbulent Air Flow Behaviour in a Rotor-Stator Cavity

Fadi Abdel Nour [a], Sébastien Poncet [b], Roger Debuchy [a], Gérard Bois [a]

a. Laboratoire de Mécanique de Lille - UMR CNRS 8107 - Arts et Métiers ParisTech
8, Boulevard Louis XIV 59046 Lille Fr
fadi_abdnour@hotmail.com , roger.debuchy@univ-artois.fr , gerard.bois@lille.ensam.fr
b. Laboratoire M2P2, UMR 6181 CNRS - Univ. Aix-Marseille,
Technopôle Château-Gombert, 38 rue F. Joliot-Curie, 13451 Marseille Fr
poncet@l3m.univ-mrs.fr

Abstract:

The present work focuses on a turbulent flow with separated boundary layers in a rotor-stator system opened to the atmosphere at the periphery, where the pre-swirl ratio of the fluid is low. Under these conditions, the fluid in the core does not always rotate as a solid body, as expected by the solution of Batchelor (1951). The experimental, theoretical and numerical results clearly explain this phenomenon.

Keywords: Rotor-Stator cavity, RANS modelling, Analytical solution, Hot-wire anemometry.

1 Introduction

Several and various researches have been carried out about turbulent flows inside rotor-stator cavities because of their high relevance to turbomachinery. One historical controversy in such configuration is due to Batchelor (1951) who proposed a model based on the presence of a rotating core between the two boundary layers and Stewartson (1953) who did not notice the solid rotation of the central core and the stator boundary layer. As far as opened rotor-stator systems are concerned, the main supplementary difficulty in finite cavity comes from the high sensitivity of the flow properties to the geometrical configuration at the periphery because of the interaction with the external domain. Djaoui et al. (1998) introduced a geometrical parameter λ based on the possible difference between the disk radii and it was shown by Debuchy et al. (2007) that the level of the pre-swirl velocity is closely linked to the variations of this parameter with the consequence that the Batchelor type flow is not always observed in a rotor-system without any superposed throughflow. The present work considers the air flow inside an annular high speed rotor-stator cavity belonging to the regime IV of Daily and Nece (1960): turbulent flow with separated boundary layers. The aim of this work is to provide comparisons between velocity measurements performed by hot-wire anemometry, numerical predictions of a second order turbulence modeling and an analytical solution.

2 Statistical Modelling

The flow presents several complexities (high rotation rate, wall effects, transition zones), which are a severe test for turbulence modelling. Our approach is based on one-point statistical modelling using a low Reynolds number second-order full stress transport closure sensitized to rotation effects (Elena and Schiestel, 1996). This approach allows for a detailed description of near-wall turbulence and is free from any eddy viscosity hypothesis. The general equation for the Reynolds stress tensor R_{ij} can be written $\dot{R}_{ij} = P_{ij} + D_{ij} + \phi_{ij} - \varepsilon_{ij} + T_{ij}$, where $\dot{R}_{ij}$ is the temporal derivative of R_{ij} and $P_{ij}, D_{ij}, \phi_{ij}, \varepsilon_{ij}, T_{ij}$ respectively denote the production, diffusion, pressure-strain correlation, dissipation and extra terms, taking into account for implicit effects of the rotation on the turbulence field.

The computational procedure is based on a finite volume method using staggered grids for mean velocity components with axisymmetry hypothesis in the mean. The computer code is steady elliptic and the numerical solution proceeds iteratively. A 140^2 mesh in the (r, z) frame proved to be sufficient in the case considered in the present work to get grid-independent solutions. The mesh is refined close to the walls: the size of the first mesh is indeed $6.89\times10^{-5}\,H$ and $7.526\times10^{-4}\,H$ in the radial and axial directions respectively.

At the wall, all the variables are set to zero except for the tangential velocity V_θ, which is set to Ωr on rotating walls and zero on stationary walls and the dissipation rate of the turbulence kinetic energy which has a finite value on all walls. In the radial gap between the stator and the hub, V_θ is supposed to vary linearly from zero on the stationary wall up to Ωr on the rotating wall. To model the opening at the periphery of the cavity, V_θ is set to zero whereas $V_r = -V_0$ on the upper part of the gap ($z^* > 0.5$) and $V_r = V_0$ on the lower part ($z^* < 0.5$). V_0 is fixed to 10% of the local disk velocity in agreement with the experimental results. Different boundary conditions have been tested (imposed pressure, zero radial velocity) but the present choice of boundary conditions provides the best results compared to the experimental data and especially it provides the good pre-swirl ratio, which is the crucial quantity for such flows as it will be shown in the following section. A weak level of turbulence is also imposed at the periphery of the cavity (see in Poncet 2005). The reader can refer to previous works by Elena and Schiestel (1996) for more details.

3 Analytical Solution

The flow takes place inside an annular cavity between a disc of radius R (rotor) rotating with an angular velocity Ω and a stationary disc (stator). The rotor-stator system has an axial gap H and is opened at the periphery. r and z denote respectively the radial and axial coordinates : $r = 0$ at the axis and $z = 0$ on the rotating wall. The significant dimensionless parameters of the problem are the axial gap ratio of the cavity $G = H/R$, the Reynolds number $Re = \Omega R^2/\upsilon$, the combination of both giving the Ekman number $Ek = 1/Re\ G^2$. The authors assumed that $G \ll 1$, $Re \gg 1$ and $Ek \ll 1$ which corresponds to turbulent flow regime with separated boundary layers.

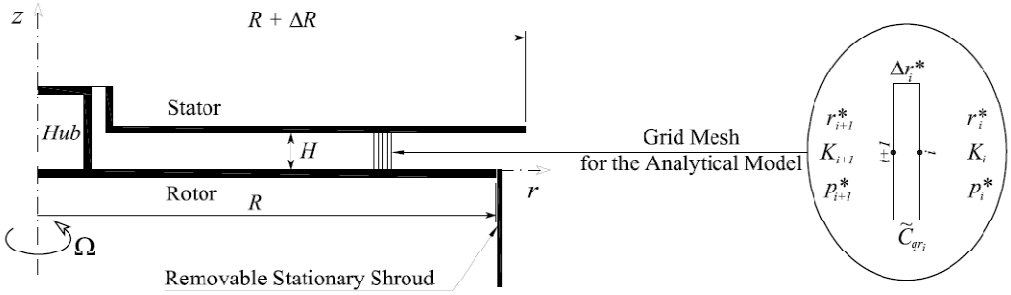

Figure 1: Schematic representation of a rotor-stator cavity

Following the theoretical approach by Debuchy et *al.* (2007), valid inside the central core flow, under assumptions of incompressible, steady and axisymmetric flow with negligible turbulence effects, the momentum equations, written in dimensionless form, are reduced to:

$$\frac{dp^*}{dz^*} = 0\ ,\ r^* V_\theta^{*2} = \frac{1}{2}\frac{dp^*}{dr^*}\ ,\ r = R\,r^*\ ,\ z = GR\,z^*\ ,\ v_\theta = \Omega r\,V_\theta^*\ ,\ p - p_{atm} = \frac{1}{2}\rho\Omega^2 R^2\,p^* \quad (1)$$

The relevant conclusion is that the dimensionless pressure p^* and tangential velocity V_θ^* are independent of z^*inside the central core, but no analytical solution can be deduced from relation (1). Additional relations can be provided starting from the dimensionless flow rate circulating inside the boundary layers estimated according to Owen and Rogers (1989) with a weighting function as introduced by Debuchy et al. (2008). The centrifugal dimensionless flow rate inside the rotor boundary layer q_R^* must be counterbalanced by a dimensionless compensation flow rate q_C^*. For a rotor-stator system with a superposed radial inflow, Debuchy et al. (2008) suggested that the dimensionless compensation flow rate q_C^* is proportional to $e^{\frac{4}{5}\varphi\, C_{qr}}\, K^{\frac{4}{5}}(r^{*2}Re)^{\frac{4}{5}}$, with the C_{qr}parameter defined by Poncet et *al.* (2005) $C_{qr} = q\,Re_r^{1/5}/(2\pi\Omega r^3)$. In the absence of any superposed flow, there is also a possible radial exchange inside the central core with the consequence that the C_{qr} parameter is to be replaced by a pseudo-dimensionless coefficient of flow rate $\widetilde{C_{qr}}$:

$$q_R^* \propto (r^{*2}Re)^{\frac{4}{5}} \quad , \quad q_C^* \propto e^{(5/4\ \varphi\ \widetilde{C_{qr}})}\, K^{\frac{4}{5}}(r^{*2}Re)^{\frac{4}{5}} \quad (2)$$

In the present work, it is assumed that the pseudo-dimensionless coefficient of flow rate $\widetilde{C_{qr}}$ is linked to the difference between the effective core swirl coefficient K and the core swirl coefficient corresponding to the

solid body rotation K_B, and also to the dimensionless radius. Consequently, assuming that $\widetilde{C_{qr}} \propto (K_B - K)\, r^{*a}$, and introducing the boundary condition $K = K_p$ at $r^* = 1$ it is found that:

$$\frac{K}{K_B} = \left(\frac{K_p}{K_B}\right)^{\left(\frac{K_B-K}{K_B-K_p}\right) r^{*a}} \tag{3}$$

The solution $K = K_B$ corresponding to a central core rotating as a solid body is obtained in the particular case $K_p = K_B$. An iterative procedure is proposed by the authors to approximate the solution for K for $K_p \neq K_B$. The domain is divided into a uniform grid with a mesh size Δr^* sufficiently small to assume that $\widetilde{C_{qr_i}}$ is quasi-invariant (Figure 1). K_{i+1} at the radial location r^*_{i+1} is computed from relation (4) using the value of K_i at the radial location $r^*_i = r^*_{i+1} + \Delta r^*_i$. This step by step process starts at $r^*_0 = 1$ where the pre-swirl coefficient is K_p. The dimensionless static pressure p^*_i at the radial location r^*_i is obtained using the following equivalent difference quotient instead of the second relation in (2), the origin of the dimensionless static pressure being $p^*_0 = 0$ at $r^*_0 = 1$:

$$\left(\frac{K_{i+1}}{K_B}\right) = \left(\frac{K_p}{K_B}\right)^{\left(\frac{K_B-K_i}{K_B-K_p}\right) r_i^{*a}}, \qquad p^*_{i+1} = p^*_i - 2\, K^2_{i+1}\, r^*_{i+1} \Delta r^*_i \tag{4}$$

4 Results and Discussion

The experimental apparatus consists of two parallel and coaxial disks separated by an adjustable inter-disk space H. The rotor and the central hub attached to it rotate at the same angular velocity Ω. For the test cases called « shrouded rotor system », the rotor was enclosed by a stationary shroud in order to minimize the perturbations brought by the centrifugal effects of the rotating walls external to the cavity. This stationary shroud was removed for the test case called « unshrouded rotor system ». Two stators were tested: the 'basic' one has the same radial dimension R as the rotor, whereas the other is slightly larger $R + \Delta R$. The present study focuses on the configuration where no superposed centrifugal or centripetal inflows are assigned. The experiments were performed within air in ambient conditions (see Debuchy et al. (2007)).

Radial and tangential velocity components and the three associated turbulent correlations were measured with a specific hot-wire probe made of two perpendicular $(5\ \mu m)$ wires situated in the same plane. Each sensor was connected to a *DANTEC 55M25* anemometry device. For each measurement, 20000 samples were recorded with a data acquisition rate fixed to $10\ KHz$.

In the present paper H was fixed to 30 mm and Ω to 1500 rpm, which corresponds to the following values of the dimensionless parameters: $Re = 1.47\ 10^6$ $(R = 375\ mm)$, $G = 0.08$ so that $Ek = 1.06\ 10^{-4}$. Two values of the geometrical parameter λ defined by $\lambda = \Delta R/H$ were tested: $\lambda = 0.0$ and $\lambda = 0.27$. In the following discussion, all results are presented in dimensionless quantity form with superscript $(*)$: $V^*_r = \frac{v_r}{\Omega r}$, $V^*_\theta = \frac{v_\theta}{\Omega r}$, $V'^{*2}_r = \frac{v'^2_r}{(\Omega r)^2}$, $V'^{*2}_\theta = \frac{v'^2_\theta}{(\Omega r)^2}$, $V'^*_r V'^*_\theta = \frac{v'_r v'_\theta}{(\Omega r)^2}$.

The first step of the discussion is based on experimental results corresponding to three distinct geometrical configurations: two values of ($\lambda = 0$ and $\lambda = 0.27$) are tested in the case of a shrouded rotor system whereas only the case $\lambda = 0.27$ is retained in the case of an unshrouded rotor system. These configurations are interesting because they lead to similar peripheral conditions as depicted in Figure 2: at $r^* = 0.976$, both tangential and radial dimensionless velocity profiles as well as the corresponding turbulent correlations are superposed. The probable reason is that the external flow structure, and consequently the peripheral inlet/outlet fluid exchange are identical for both configurations. Figure 2 shows that, at this radial location $r^* = 0.976$, the radial velocity profile is divided into two zones: the flow is directed inward on the stator side for $0.5 \leq z^* \leq 1$ and it is ejected under the centrifugal effects of the rotating wall for $z^* \leq 0.5$. It means that a radial circulation outside the boundary layers does exist. Figure 2b reveals that the tangential velocity profile is divided into three distinct zones: the two boundary layers adjacent to the disks wall in which the axial gradients of velocity are important because of the adherent conditions to the walls and a central core in which the tangential velocity is nearly independent of the axial position z. Note that the level of the pre-swirl (i.e. the dimensionless tangential velocity at $r^* = 0.976$ and $z^* = 0.5$) is around 0.22. Figures 2 c-e show that the turbulence intensities are very weak.

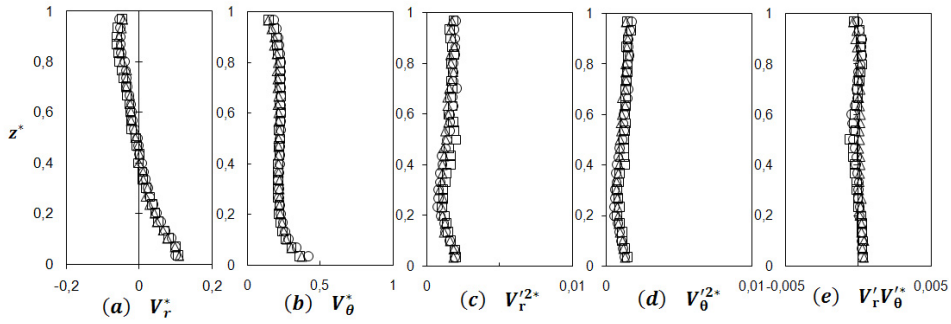

Figure 2: Experimental results at $r^* = 0.976$.
Shrouded rotor system: o $\lambda = 0$; □ $\lambda = 0.27$; Unshrouded rotor system: Δ $\lambda = 0.27$.

Figure 3 brings to light that for $r^* = 0.773$, the radial velocity profiles are again divided into two zones whereas the radial exchange of fluid in the core region gradually vanishes as the local radius decreases. For $r^* = 0.613$, the radial flow circulates only through the boundary layers. The tangential velocity profile is divided into 3 distinct zones, as previously described, for all radii in the range $0.427 \leq r^* \leq 0.880$. The level of the dimensionless tangential velocity in the central core is a decreasing function of r^*as if there is a centripetal superposed flow, until it reaches a nearly constant value for $r^* \leq 0.533$: the central core flow rotates as a solid body with a velocity approximately equals to $0.38 - 0.40$ of the local velocity of the rotating disk.

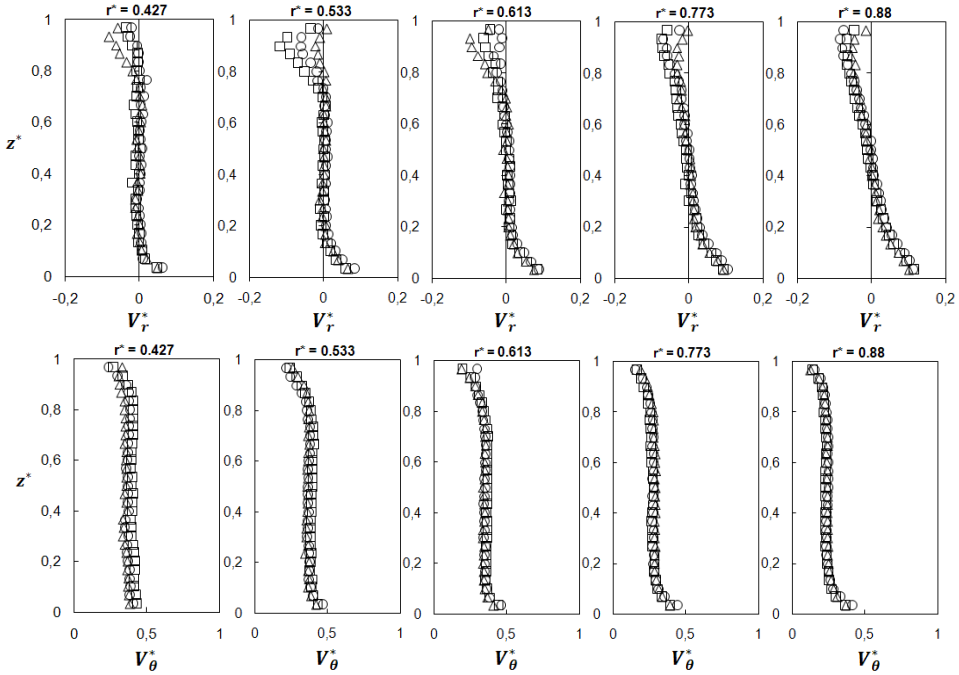

Figure 3: Axial profiles of the mean radial and tangential velocity components at various radii. See legend of Figure 2.

The second step of the discussion deals with comparison between experiments and numerical results. As the three different geometry arrangements at the periphery of the cavity give nearly the same flow properties, the numerical results have been compared only to experimental data in the unshrouded case for $\lambda = 0.27$. Figure 4 shows comparisons for the mean radial and tangential velocity components for radii in the range $0.427 \leq z^* \leq 0.880$. The RSM model reproduces well the flow structure especially at the periphery of the cavity. The tangential velocity profile is divided into three distinct zones for all values of r^*, whereas the radial velocity profile is divided into two zones near the periphery at $r^* = 0.880$, and into three zones closer to the rotation axis. When r^* decreases, note the transition to the Batchelor flow structure for $r^* \leq 0.6$. both visible in the experimental data and in the numerical results There is an excellent agreement between the two approaches for the mean field. The Ekman layer along the rotor is well reproduced by the model as well as the core-swirl ratio. A small discrepancy is observed along the stator, where the RSM model tends to underestimate the thickness of the Bödewadt layer.

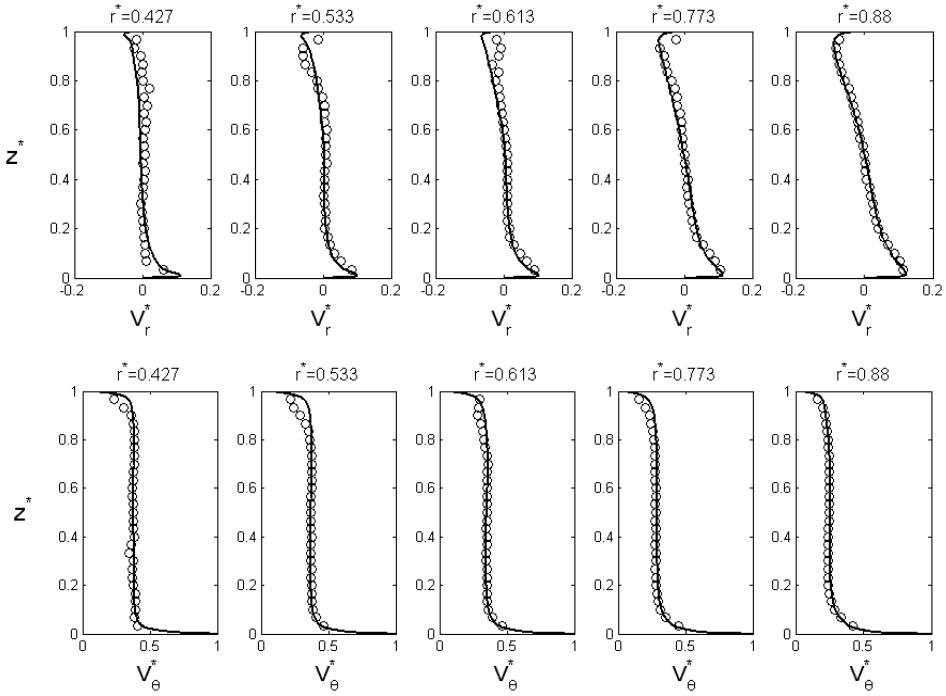

Figure 4: Axial profiles of the mean radial and tangential velocity component. Comparison between experiments (o) and numerical results (lines).

The numerical results are compared to the velocity measurements for the three associated Reynolds stress components at one radial location $r^* = 0.773$ (Figure 5). The cross component is quite weak compared to the two normal components. Turbulence is mainly concentrated in the boundary layers but, contrary to the case of turbulent flows in a closed cavity, the central core is turbulent too. Thus, turbulence intensities slightly vary with the axial position. The RSM model predicts quite well the turbulent field apart very close to the stator, where the normal turbulence intensities are slightly underestimated. These weak discrepancies may be attributed to both the difficulty to acquire measurements close to this wall but also to the choice of the boundary conditions at the periphery of the cavity in the modeling.

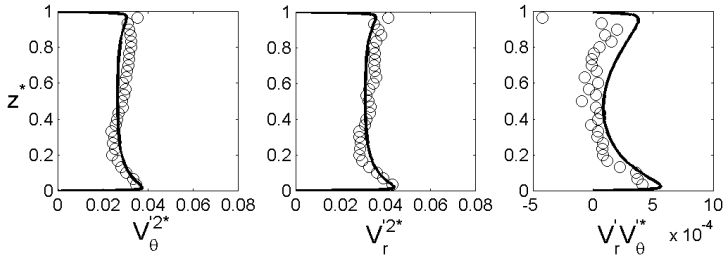

Figure 5: Axial profiles of three components of the Reynolds stress tensor at $r^* = 0.773$. Comparison between experiments (o) and numerical results (lines).

Figure 6 presents the radial distributions of the core-swirl ratio. The theoretical distribution deduced from formula (4) with $K_B = 0.382, K_p = 0.22, a = 0.65$ is in good agreement with the numerical results and the velocity measurements for this range of radial location. The dimensionless tangential velocity level in the central core increases when approaching the rotation axis to reach a value close to 0.382 for $r^* = 0.40$. It is to be compared to the value 0.438 obtained experimentally and analytically by Poncet *et al.* (2005a) for turbulent flows in an enclosed cavity. This variation can be clearly attributed to the opening at the periphery, which strongly modifies the inlet/outlet conditions and especially the level of the core swirl ratio, which is around 0.24 for $r^* = 0.9$ in the RSM model, very close to that obtained for the unshrouded rotor cavity for the $(\lambda = 0.27)$ case.

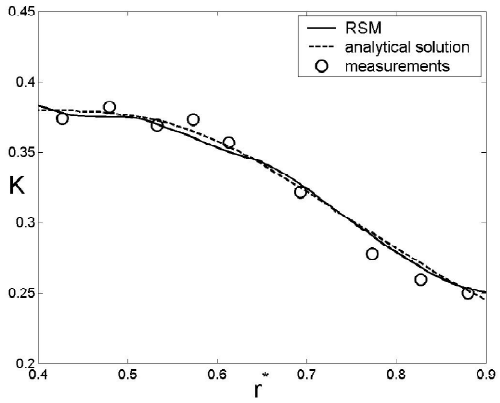

Figure 6: Radial distributions of the core-swirl ratio.
Comparison between experiments (o) numerical results (line) and theory (dashed line).

5 Conclusion

Measurements, theoretical and numerical modelling of the turbulent flow in a rotor-stator cavity is a great challenge even more when the cavity is opened to the atmosphere at the periphery. In the present work, we have compared extensive velocity measurements for configurations leading to the same value of the pre-swirl ratio equal to 0.22 and to very weak turbulence intensities around the opening. The experimental results have been used as boundary conditions in the numerical modelling. The second order model results agree well with the experimental data for both the mean and turbulent fields. The thicknesses of the boundary layers as well as the core-swirl ratio are well predicted at all radial locations. A weak discrepancy is observed along the stator, where the RSM model slightly under predicts the Bödewadt boundary layer thickness. The radial distribution of the core swirl ratio K is also well predicted by a new analytical solution valid in the central core. The main result of this work is that the flow structure and especially the core-swirl ratio, which is the most interesting quantity for turbomachinery application, depend exclusively on the pre-swirl ratio and on the weak inward/outward radial flow at the opening.

References

[1] Batchelor G.K. (1951). Note on a class of solutions of the Navier–Stokes equations representing steady rotationally-symmetric flow, J. Mech. Appl. Math. 4, 29-41.
[2] Daily J.W. and Nece R.E. (1960). Chamber dimension effects on induced flow and frictional resistance of enclosed rotating disks. ASME J. Basic Eng. 82, 217-232.
[3] Debuchy R., Abdel Nour F., & Bois G. (2008). On the flow behavior in rotor-stator system with superposed flow. International Journal of Rotating Machinery, 2008, 10.1155/2008/719510.
[4] Debuchy R., Della Gatta S., D'Haudt E., Bois G., Martelli F. (2007). Influence of external geometrical modifications on the flow behavior of a rotor-stator system: numerical and experimental investigation, Proceedings of the I MECH E Part A Journal of Power and Energy 221 (6), 857-863.
[5] Djaoui M., Malesys A., Debuchy R., (1998). Mise en évidence expérimentale de la sensibilité de l'écoulement de type rotor-stator aux effets de bord, C.R. Acad. Sci. Paris Série II b, t.327, 49-54.
[6] Elena L. and Schiestel R., (1996). Turbulence modelling of rotating confined flows, Int. J. Heat Fluid Flow 17, 283-289.
[7] Owen, J.M. & Rogers, R.H. (1989). Flow and heat transfer in rotating-disc system: Vol.1 Rotor-stator system. Ed.W.D.Morris, John Wiley & Sons Inc.
[8] Poncet S. (2005). Ecoulements de type rotor-stator soumis à un flux axial : de Batchelor à Stewartson, PhD thesis, University of Aix-Marseille 1.
[9] Poncet S., Chauve M.P., Le Gal P. (2005a). Turbulent Rotating Disk Flow with Inward Throughflow, J. Fluid Mech. 522, 253-262.
[10] Poncet S., Chauve M.P., Schiestel R. (2005b). Batchelor versus Stewartson flow structures in a rotor-stator cavity with throughflow, Phys. Fluids 17, 075110.
[11] Stewartson K. (1953). On the flow between two rotating coaxial discs, Proc.Camb.Phil.Soc. 49, 333-341.